



Research Article

# Highly Selective Au/ZnO via Colloidal Deposition for CO<sub>2</sub> Hydrogenation to Methanol: Evidence of AuZn Role

Hasliza Bahruji<sup>1,\*</sup>, Mshaal Almalki<sup>2</sup>, Norli Abdullah<sup>3</sup>

<sup>1</sup>Centre of Advanced Material and Energy Science, University Brunei Darussalam, Jalan Tungku Link, BE 1410, Brunei Darussalam.

<sup>2</sup>Department of Chemistry, Imam Abdul Rahman Bin Faisal University, Dammam, Saudi Arabia.

<sup>3</sup>Studies, Universiti Pertahanan Nasional Malaysia, Kem Sungai Besi, 57000, Kuala Lumpur, Malaysia.

Received: 18<sup>th</sup> November 2020; Revised: 19<sup>th</sup> January 2021; Accepted: 19<sup>th</sup> January 2021  
Available online: 15<sup>th</sup> March 2021; Published regularly: March 2021



## Abstract

Gold, Au nanoparticles were deposited on ZnO, Al<sub>2</sub>O<sub>3</sub>, and Ga<sub>2</sub>O<sub>3</sub> via colloidal method in order to investigate the role of support for CO<sub>2</sub> hydrogenation to methanol. Au/ZnO was also produced using impregnation method to investigate the effect of colloidal method to improve methanol selectivity. Au/ZnO produced via sol immobilization showed high selectivity towards methanol meanwhile impregnation method produced Au/ZnO catalyst with high selectivity towards CO. The CO<sub>2</sub> conversion was also influenced by the amount of Au weight loading. Au nanoparticles with average diameter of 3.5 nm exhibited 4% of CO<sub>2</sub> conversion with 72% of methanol selectivity at 250 °C and 20 bar. The formation of AuZn alloy was identified as active sites for selective CO<sub>2</sub> hydrogenation to methanol. Segregation of Zn from ZnO to form AuZn alloy increased the number of surface oxygen vacancy for CO<sub>2</sub> adsorption to form formate intermediates. The formate was stabilized on AuZn alloy for further hydrogenation to form methanol. The use of Al<sub>2</sub>O<sub>3</sub> and Ga<sub>2</sub>O<sub>3</sub> inhibited the formation of Au alloy, and therefore reduced methanol production. Au/Al<sub>2</sub>O<sub>3</sub> showed 77% selectivity to methane, meanwhile Au/Ga<sub>2</sub>O<sub>3</sub> produced 100% selectivity towards CO.

Copyright © 2021 by Authors, Published by BCREC Group. This is an open access article under the CC BY-SA License (<https://creativecommons.org/licenses/by-sa/4.0>).

**Keywords:** Au nanoparticles; ZnO catalyst; CO<sub>2</sub> hydrogenation; methanol

**How to Cite:** Bahruji, H., Almalki, M., Abdullah, N. (2021). Highly Selective Au/ZnO via Colloidal Deposition for CO<sub>2</sub> Hydrogenation to Methanol: Evidence of AuZn Role. *Bulletin of Chemical Reaction Engineering & Catalysis*, 16(1), 44-51 (doi:10.9767/bcrec.16.1.9375.44-51)

**Permalink/DOI:** <https://doi.org/10.9767/bcrec.16.1.9375.44-51>

## 1. Introduction

Methanol production is growing rapidly to sustain industrial demand, for example as starting material in biodiesel and fuel productions, also as solvent in pharmaceutical and cosmetic industries. Methanol has also been recognized as potential clean energy carrier in comparison to hydrogen and natural gas mainly due to the

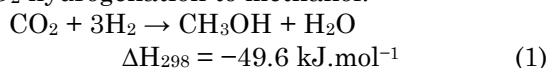
nature of methanol as liquid fuel, which is convenient during transportation and storage [1]. Methanol is currently produced via hydrogenation of synthetic gas (CO + H<sub>2</sub>) on Cu/ZnO/Al<sub>2</sub>O<sub>3</sub> catalysts, with the addition of CO<sub>2</sub> to increase the productivity [2]. Synthetic gas was originated from reforming of natural gas with water at high temperatures to form a mixture of CO and H<sub>2</sub> [3]. The concern associated with the sustainability of natural gas has prompted investigation to find alternative carbon feedstock for methanol production.

\* Corresponding Author.

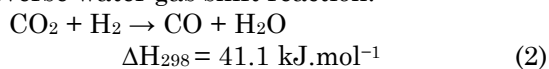
Email: [hasliza.bahruji@ubd.edu.bn](mailto:hasliza.bahruji@ubd.edu.bn) (H. Bahruji);

Investigation on methanol production from CO<sub>2</sub> has attracted significant interests in the recent years as pathway to mitigate the rising level of CO<sub>2</sub> in the atmosphere [4,5]. The CO<sub>2</sub> hydrogenation to methanol provides a viable and sustainable approach for methanol synthesis. The use of CO<sub>2</sub> as carbon feedstock also offers utilization of greenhouse gas to be converted into a value added commodity [6]. Methanol is thermodynamically favored product from CO<sub>2</sub> hydrogenation reaction at low temperature and high pressure conditions [7]. At high temperature, CO<sub>2</sub> undergoes reverse water gas shift reaction to CO, thus reducing the selectivity towards methanol. CO can also be produced from decomposition of resulting methanol to CO.

CO<sub>2</sub> hydrogenation to methanol:



Reverse water gas shift reaction:



Active catalysts required metal sites for hydrogen dissociation, C–O bond activation and stabilization of intermediate formate species during the catalytic conversion of CO<sub>2</sub> to methanol [8]. Palladium and copper have been mostly investigated for CO<sub>2</sub> hydrogenation to methanol, with most studies suggested the importance of Pd and Cu oxidation state in enhancing methanol production [9-11]. Metal nanoparticles that was highly distributed onto metal oxides support increased the CO<sub>2</sub> conversion to methanol [12]. Studies on Au catalyst for CO<sub>2</sub> hydrogenation has been reported previously indicating the activity was strongly affected by the support [13]. Au/ZnO exhibited high selectivity for methanol production, with significantly low activity towards reserves water gas shift reaction [11]. The presence of surface vacancy on ZnO also modified the charge state of the Au nanoparticles, consequently influenced the activity of Au/ZnO catalysts [14].

Catalysts with high activity towards methanol production can be achieved by increasing dispersion of nanoparticles on metal oxide support. Here in this work we investigate the influence of Au nanoparticles deposited via colloidal method on different metal oxide support for CO<sub>2</sub> hydrogenation to methanol. The catalytic performance of Au/ZnO catalyst was also compared with Au/ZnO produced by impregnation. Au was deposited Al<sub>2</sub>O<sub>3</sub> and Ga<sub>2</sub>O<sub>3</sub>, in order to elucidate the role of ZnO in enhancing methanol production.

## 2. Materials and Methods

### 2.1 Catalysts Preparation

Catalysts were prepared using incipient wetness impregnation method and sol immobilization of Au colloid on ZnO. For impregnation, HAuCl<sub>4</sub> solution was added drop-wisely onto ZnO and the mixture was ground to form a paste. The paste was dried in air oven at 120 °C followed by calcination in air at 500 °C. Catalyst was also prepared using sol immobilization method in which the Au nanoparticles were prepared via reduction with NaBH<sub>4</sub> and using polyvinyl alcohol as nanoparticles stabilizer. The resulting Au nanoparticles were deposited onto ZnO by reducing the pH of the solution to 2 with HCl. The amount of Au metal deposited onto ZnO was varied at 1 %wt and 5 wt% loading. The resulting Au/ZnO were used for methanol production via hydrogenation of CO<sub>2</sub>. The process was repeated using Al<sub>2</sub>O<sub>3</sub> and Ga<sub>2</sub>O<sub>3</sub>.

### 2.2 Catalyst Characterizations

The structural properties of Au nanoparticles were characterized using XRD, XPS, TEM, SEM and EDX. XRD were obtained at room temperature using an Enraf Nonus FR590 diffractometer fitted with a hemispherical analyzer, using Cu-K $\alpha$  radiation (1/4 1.54 Å) and analyzed using X-pert HighScore. X-ray photoelectron spectra (XPS) were recorded using Kratos Axis Ultra-DLD XPS spectrometer with a monochromatic Al K $\alpha$  source (75–150 W) and analyzer pass energies of 160 eV (for survey scans) or 40 eV (for detailed scans). Data were analyzed using Casa XPS software. The morphological analysis was carried out using JEOL 2100 (LaB6) high-resolution transmission electron microscope (HRTEM) system fitted with a high-resolution Gatan digital camera (2k 2k) and a dark held HAADF/Z-contrast detector. Samples were suspended in DI water and *ca.* 1  $\mu$ L was added to the TEM grid and dried. SEM-EDX analysis was also carried out to determine elemental composition of the catalysts.

### 2.3 Catalytic Activity for CO<sub>2</sub> Hydrogenation

Catalytic testing for CO<sub>2</sub> hydrogenation was carried out in a fixed-bed continuous-flow reactor shown in Figure 1. 0.5 g of catalyst was placed in a stainless tube reactor and was pre-reduced in a flow of 5 % H<sub>2</sub>/Ar gas (30 mL/min) for 1 h at 400 °C. The reactor was cooled to 250 °C and a mixture of CO<sub>2</sub> and H<sub>2</sub> gases, (1 CO<sub>2</sub>: 3 H<sub>2</sub> molar ratios) was introduced with a flow rate of 30 mL.min<sup>-1</sup>. The pressure was in-

creased to 20 bar using a back-pressure valve. All the post-reactor lines and valves were heated at 130 °C to avoid product condensation. The gas products were analyzed using gas chromatography with (Clarus 450). Methanol was analyzed using an Elite WAX ETR column and FID detector. The CO<sub>2</sub>, H<sub>2</sub>, and CO gases were analyzed using Carboxen-1000 column with TCD detector. Reported values are given after 3 h of reaction under steady state unless otherwise stated.

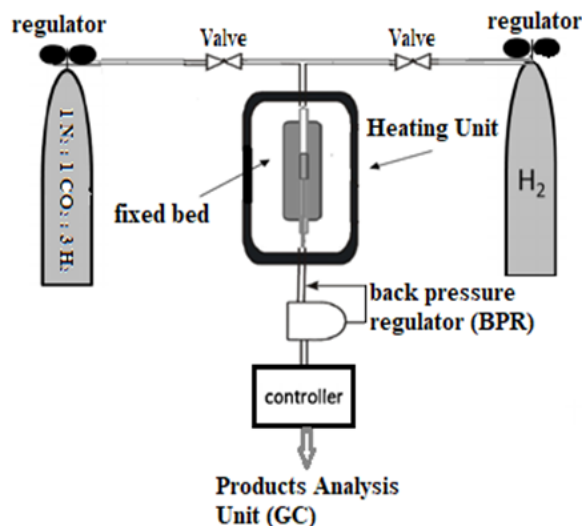


Figure 1. Reactor diagram for CO<sub>2</sub> hydrogenation reaction.

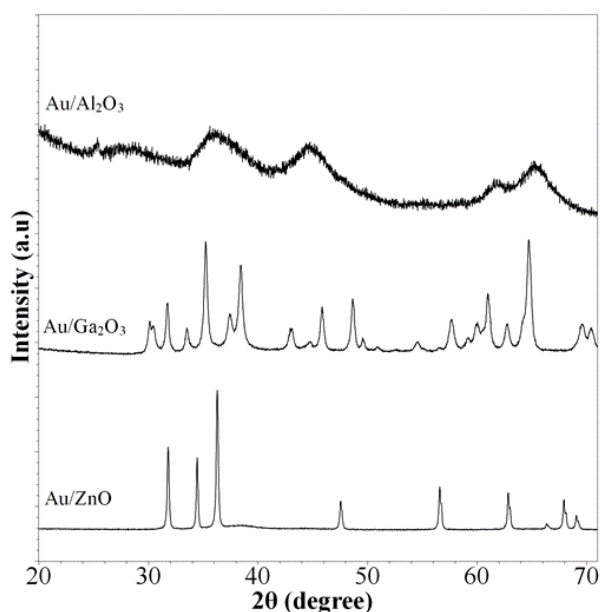


Figure 2. X-ray diffractogram of 5% Au/ZnO, 5% Au/Ga<sub>2</sub>O<sub>3</sub> and 5% Au/Al<sub>2</sub>O<sub>3</sub> catalysts prepared using sol immobilization 30(401), 31(002).

### 3. Results and Discussions

#### 3.1 Catalysts Characterizations

All catalysts were characterized using XRD after drying in air and following reduction in H<sub>2</sub> gas at 400 °C for 1 h. As shown in Figure 2, the peaks appeared at  $2\theta = 31.7^\circ, 34.4^\circ, 36.2^\circ, 47.5^\circ, 56.5^\circ, 62.8^\circ, 66.3^\circ, 67.9^\circ,$  and  $69.0^\circ$  corresponding to the characteristic ZnO crystal planes of (100), (002), (101), (102), (110), (103), (200), (112), and (201). The diffraction pattern was consistent with the hexagonal phase of ZnO (JCPDS No. 79-2205). Closed observation on the diffraction angle region between  $37^\circ$ – $46^\circ$  revealed the diffraction pattern of Au nanoparticles after drying at 120 °C. The Au(111) peak appeared as a small hump centered at  $38.5^\circ$  indicating the presence of high dispersed Au nanoparticles on ZnO [15]. XRD analysis of Au/Al<sub>2</sub>O<sub>3</sub> showed the broad peaks appeared at  $37^\circ$  (311),  $46^\circ$  (400),  $62^\circ$  (511) and  $66^\circ$  (440) corresponded to  $\gamma$ -Al<sub>2</sub>O<sub>3</sub> (JCPDS no 50-0741). XRD analysis of Au/Ga<sub>2</sub>O<sub>3</sub> showed the peaks corresponded to  $\beta$ -Ga<sub>2</sub>O<sub>3</sub> (JCPDS no. 76-0573). The Au peak at  $38.8^\circ$  in Au/Al<sub>2</sub>O<sub>3</sub> and Au/Ga<sub>2</sub>O<sub>3</sub> was absent in the XRD due to the overlapping of Au peak with the metal oxides diffraction peaks.

Figure 3 showed the XRD analysis of Au/ZnO within  $37^\circ$ – $46^\circ$  in order to clearly indicate the presence of Au nanoparticles. Following reduction at 400 °C, the peak associated to Au(111) crystalline plane showed an increase in intensity with a sharp peak appeared at  $38.8^\circ$ . A small peak appeared at  $39.6^\circ$  which indicates the formation of AuZn alloy [16,17]. Re-

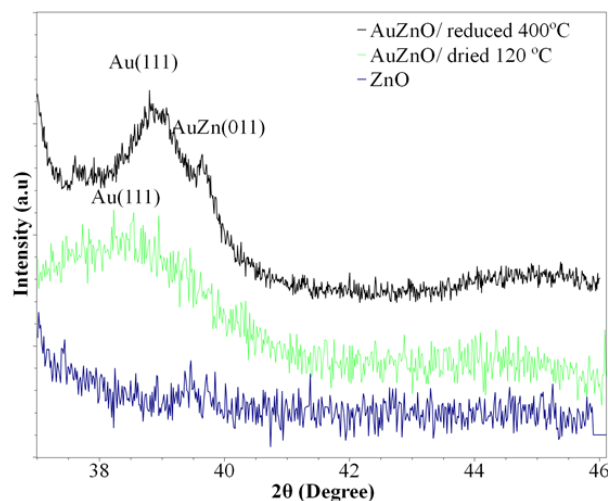
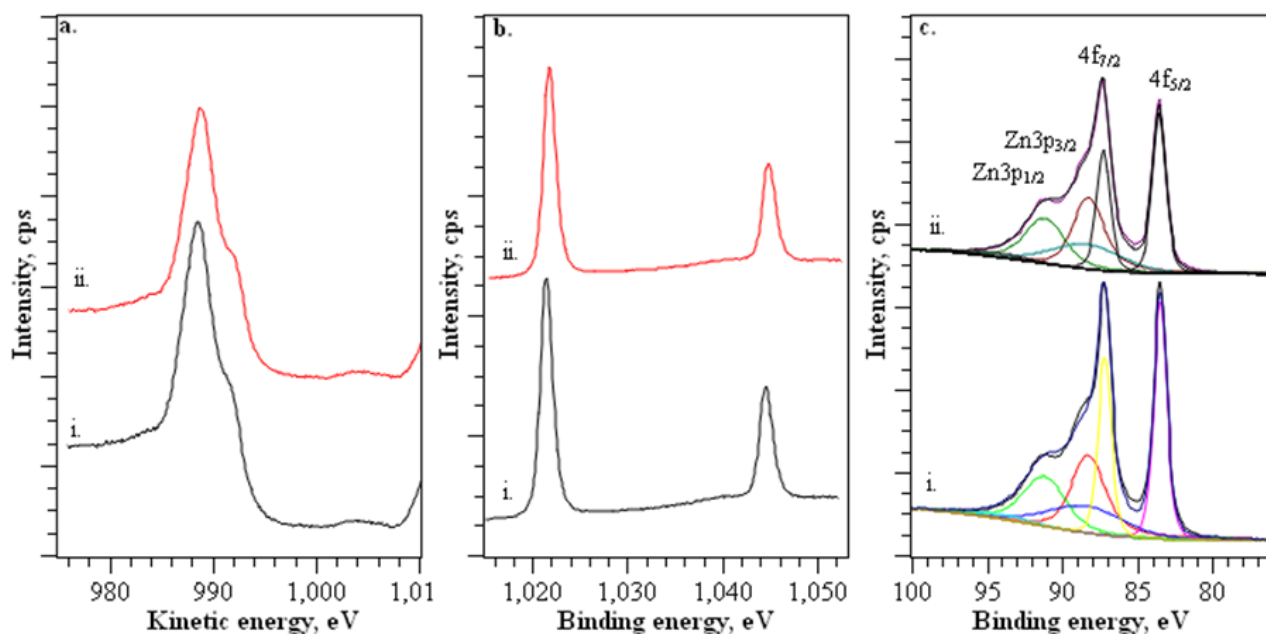


Figure 3. Closed observation on the diffraction patterns within  $37^\circ$ – $46^\circ$  of ZnO (–), 5% Au/ZnO dried at 120 °C (–), and 5% Au/ZnO reduced in H<sub>2</sub> gas at 400 °C (–).

duction of Au/ZnO at 400 °C reduced the ZnO within Au perimeter via hydrogen atom spill over. The Zn was migrated onto Au surface to form AuZn alloy.

To obtain further understanding into surface characteristic of Au/ZnO, X-ray photoelectron spectroscopy (XPS) was applied to examine the chemical state and surface composition. The XPS spectra of 5% Au/ZnO following reduction in hydrogen at 400 °C was compared to the fresh catalyst after drying in air at 120 °C. The spectra was calibrated to the C 1s signal at

284.8 eV. Figure 4a showed the XP spectra of Zn L<sub>3</sub>M<sub>24</sub>M<sub>24</sub> Auger electron, with peak associated to ZnO at 988.5 eV was observed. No significant differences between the catalysts before reduction and after annealing in hydrogen gas at 400 °C. Although the formation of AuZn alloy was observed from XRD, the negligible evident of Zn alloying in XPS signal due to the domination of zinc oxide on the surface of the catalyst. Studies on the changes in Zn L<sub>3</sub>M<sub>24</sub>M<sub>24</sub> Auger spectra for PdZn alloy showed the Zn alloy signal appeared as a shoulder



**Figure 4.** XPS analysis of 5% Au/ZnO i. dried at 120 °C and ii. Reduced in H<sub>2</sub> at 400 °C; a. XPS Zn LMM Auger electron spectra; b. XPS Zn 2p<sub>3/2</sub> spectra and c. XPS Au 4f spectra.

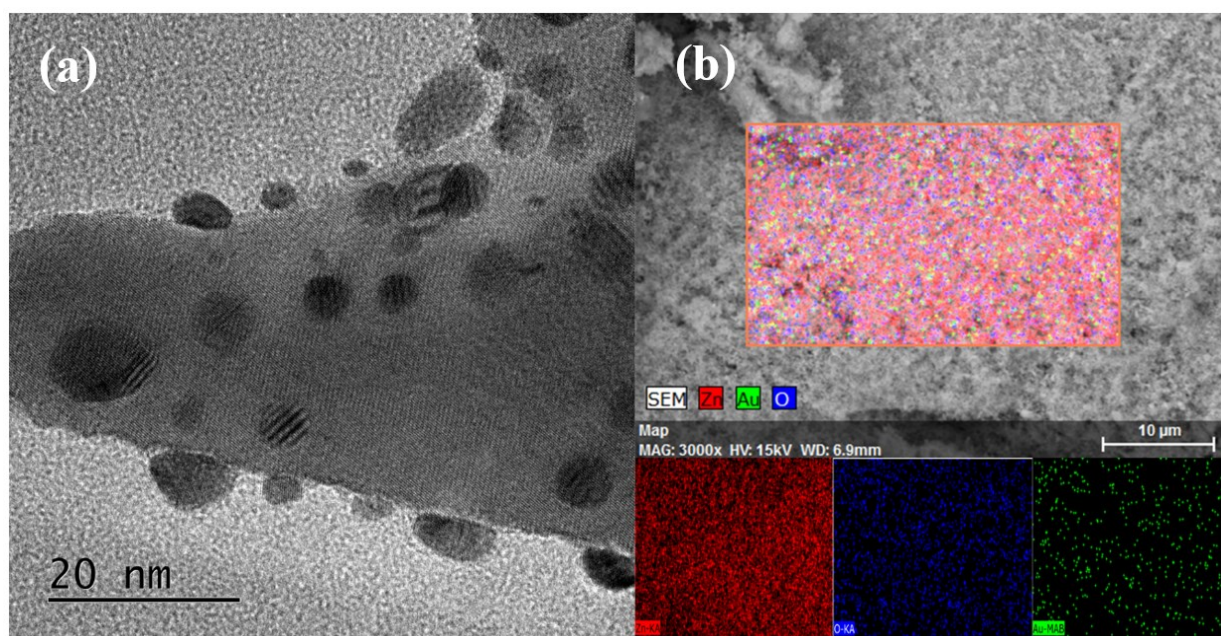


**Figure 5.** TEM image (a) and SEM-EDX analysis of 5% Au/ZnO catalyst (b).

peak at 991 eV that reflect the changes in the M (valence) levels of Zn [10]. This observation was negligible in 5% Au/ZnO, in relation to the XRD data, the Au was predominantly existed as Au monometallic. The Zn 3p<sub>3/2</sub> spectra also showed similar observation as the Zn L<sub>3</sub>M<sub>24</sub>M<sub>24</sub> signal, that only peaks associated to ZnO were observed at 1022 eV and 1045 eV. XPS Au 4f spectra of 5% Au/ZnO showed peaks of Zn 3p<sub>3/2</sub> and Zn 3p<sub>1/2</sub> (at 89 and 91.9 eV, respectively) overlapping to the two-distinct spin-orbit pairs 4f<sub>5/2</sub> at 88eV and 4f<sub>7/2</sub> 84.4eV corresponding to Au<sup>0</sup>, which further confirms the formation of Au<sup>0</sup> NPs [18]. There were no significant differences between the drying and annealing treatment in hydrogen of the XPS Au 4f spectra of 5% Au/ZnO.

TEM was applied to characterize the morphology of the catalysts, and especially to gain the particle size distribution of Au nanoparticles. The catalyst was reduced at 400 °C in hydrogen flow for 1 h prior to analysis. Surface morphology of 5% Au/ZnO was also analyzed using Scanning Electron Microscopy (SEM) and the elemental composition was determined using energy-dispersive X-ray (EDX) analysis techniques. Figure 5 showed the TEM image of 5 Au %wt of supported ZnO. The average particle size was obtained by measuring the diameter of Au nanoparticles in ten different TEM images of the catalyst. Au nanoparticles were evenly distributed on the ZnO support with average diameter of 3.5 nm. The SEM-EDX analysis shown in Figure 5b identified the presence of Au nanoparticles on ZnO support with elemental analysis carried out by EDX indicates the presence of 4.88 %wt of Au.

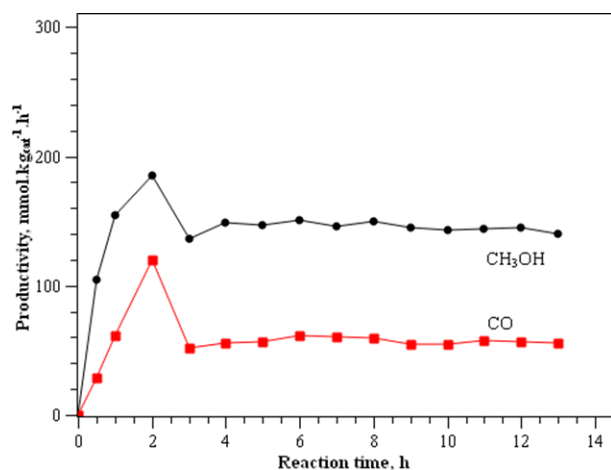


**Figure 6.** Plot of methanol and CO productivity over 13 h of CO<sub>2</sub> hydrogenation reaction at 20 bar and 250 °C using 5% Au/ZnO prepared via sol immobilization.

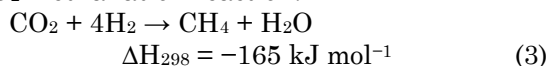
### 3.2 Catalytic Activity

CO<sub>2</sub> hydrogenation reaction was carried out on the catalysts under the flow of 3H<sub>2</sub>:1CO<sub>2</sub> gasses mixtures with N<sub>2</sub> was used as internal standard. The conversion of CO<sub>2</sub> was calculated for every 30 minutes of reaction by sampling the outlet gas via online gas chromatography analysis. In this study the reaction was kept at 250 °C based on our previous work on CO<sub>2</sub> hydrogenation on PdZn catalysts that indicated the optimum reaction condition was achieved at 250 °C and 20 bar [10,12,19,20]. The reaction was carried out for 13 h to study the stability of the 5% Au/ZnO catalyst in the presence of resulting water at high temperature and pressure. Catalytic reaction was evaluated at 20 bar of pressure, in which the condition was relatively mild in comparison to the industrial application for methanol production, normally required pressure at 50 bar. The activation of CO<sub>2</sub> required temperature at more than 200 °C, however increasing the temperature may also increase the formation of CO due to reverse water gas shift reaction [21]. Control experiment was conducted on blank reactor and on ZnO only as catalysts. For both conditions, only traces amount of CO and methanol were detected that were less than 0.1% conversion.

The calculated CH<sub>3</sub>OH and CO productions were plotted against reaction time as shown in Figure 6. The production of methanol and CO were fluctuated at the beginning of the reaction before reached steady state at 3 h. The catalyst showed stable activity with the production of methanol was determined at ~144.9 mmol/kg.h during 13 h of reaction. CO was also produced at 56.3 mmol/kg.h which was at much slower rate than methanol. The formation of methanol and CO indicated that Au nanoparticles deposited on ZnO via sol immobilization was active to drive CO<sub>2</sub> hydrogenation reaction at mild reaction condition. The catalyst produced 4% of CO<sub>2</sub> conversion with selectivity towards methanol reached 72%, and CO was produced at 28% of selectivity. The catalyst was stable towards deactivation for 13 h of reaction with no traces of methane was detected. The results were in contrast to Au/Al<sub>2</sub>O<sub>3</sub> catalysts that exhibited ~98% selectivity to methane, and also Au/Ga<sub>2</sub>O<sub>3</sub> with 100% selectivity to CO (Table 1). Methane was formed from CO<sub>2</sub> methanation reaction in the presence of moderate basic catalysts, such as: Na-Y [22] and Al<sub>2</sub>O<sub>3</sub> [23]. CO<sub>2</sub> underwent two C–O dissociations to form carbon atom, and further hydrogenated to produce methane. The use of Ga<sub>2</sub>O<sub>3</sub>

as support was suggested to prevent stabilization of formate as intermediate species during CO<sub>2</sub> hydrogenation reaction, therefore resulting in further decomposition to CO.

CO<sub>2</sub> methanation reaction:



The formation of AuZn alloy as evidenced from XRD analysis was suggested play the role of active center in methanol production. The segregation of Zn from ZnO to form AuZn alloy during reduction at 400 °C created surface vacancy on ZnO. CO<sub>2</sub> adsorbed on ZnO surface vacancy to form formate intermediates [24]. Formate can be stabilized for further hydrogenation to methanol, or decomposed to form CO and H<sub>2</sub>O. Although, currently there is no spectroscopy studies to show the stabilization of formate on AuZn alloy, the nature of formate to form bidentate formation on the metal surface via two oxygen atoms was suggested to be stabilized by AuZn alloy species. The low coordinated Au atom that was able to stabilize CO molecules was also decreased with the formation of AuZn alloy, thus limiting the reverse water gas shift reaction [16].

The activity of Au/ZnO catalyst was also investigated by reducing the amount of Au loading to only 1 %wt. The catalyst was prepared using similar sol immobilization method. The catalytic performance of 1 %wt. Au/ZnO was carried out at similar reaction conditions with the results were summarized in Table 1. The CO<sub>2</sub> conversion was significantly reduced in comparison to 5%/Au/ZnO with only 1.8% of CO<sub>2</sub> conversion. The selectivity of methanol however was approximately similar at ~79% with total production of methanol was ~66.7 mmol/kg.h. Variation of Au weight loading on ZnO metal oxide support revealed the importance of Au nanoparticles to provide active

sites for CO<sub>2</sub> hydrogenation reaction. Increasing the Au loading enhanced the number of sites for CO<sub>2</sub> activation and hydrogenation and therefore improved the CO<sub>2</sub> conversion and methanol productivity. It is also interesting to see that the Au catalyst produced via sol immobilization regardless of the metal weight loading showed comparable selectivity towards methanol production. The catalytic performance of Au nanoparticles via sol immobilization was also compared to the 1 %wt. Au/ZnO catalyst that was prepared using incipient wetness impregnation method (Table 1). The Au/ZnO produced using impregnation method appeared less active with only 0.9% of CO<sub>2</sub> conversion. The selectivity towards methanol was also reduced to only 39% to give 16.5 mmol/kg.h of methanol. The selectivity of CO was significantly higher on Au/ZnO produced via impregnation and dominating the catalytic reaction to give 25.3 mmol/kg.h of CO productivity.

#### 4. Conclusions

Au nanoparticles deposited on ZnO support via colloidal method showed high selectivity towards methanol at mild reaction conditions. Reduction of Au/ZnO at 400 °C produced AuZn alloy responsible for CO<sub>2</sub> hydrogenation to methanol. Au showed a narrow size distribution on ZnO to give 3.5 nm of average nanoparticles size. Increasing the Au weight loading from 1% to 5% on ZnO significantly enhanced CO<sub>2</sub> conversion and methanol production, although the selectivity towards methanol is remained similar regardless of the amount of Au loading. High selectivity of methanol was observed on Au catalysts produced from colloidal method meanwhile impregnation of Au produced catalyst that favored CO production. High selectivity towards methane on Au/Al<sub>2</sub>O<sub>3</sub> and CO on Au/Ga<sub>2</sub>O<sub>3</sub> indicated the important of AuZn alloy for formation of methanol. The re-

**Table 1.** Catalytic performance of 5% Au/ZnO, 5% Au/Al<sub>2</sub>O<sub>3</sub>, 5% Au/Ga<sub>2</sub>O<sub>3</sub> and 1% Au/ZnO prepared using sol immobilization; and 1% Au/ZnO prepared using impregnation method on CO<sub>2</sub> hydrogenation reaction at 20 bar and 250 °C.

Catalyst	Method	$\chi_{\text{CO}_2}$ (%)	$S_{\text{CH}_3\text{OH}}$ (%)	$S_{\text{CO}}$ (%)	$S_{\text{CH}_4}$ (%)	CH <sub>3</sub> OH (mmol.kg <sub>cat</sub> <sup>-1</sup> .H <sup>-1</sup> )	CO (mmol.kg <sub>cat</sub> <sup>-1</sup> .H <sup>-1</sup> )	CH <sub>4</sub> (mmol.kg <sub>cat</sub> <sup>-1</sup> )
1%Au/ZnO	CM <sup>a</sup>	1.8±0.2	79	20	0	66.7	16.8	0
1%Au/ZnO	IM <sup>b</sup>	0.9±0.1	39	60	0	16.5	25.3	0
5%Au/ZnO	CM <sup>a</sup>	4.3±0.2	72	28	0	144.9	56.3	0
5%Au/Al <sub>2</sub> O <sub>3</sub>	CM <sup>a</sup>	2.2±0.2	0	3.8	96.2	0	23.5	596
5%Au/Ga <sub>2</sub> O <sub>3</sub>	CM <sup>a</sup>	0.5±0.1	0	100	0	0	27.0	0

<sup>a</sup>Colloidal method; <sup>b</sup>Impregnation method.

sults suggested Au nanoparticles on ZnO support with uniform size and distribution were obtained from colloidal method, produced highly selective catalysts towards methanol at mild reaction conditions.

### Acknowledgements

Authors would like to acknowledge University Brunei Darussalam (UBD University Research Grant (UBD/RSC/URC/RG(b)/2019/012)) for financial support to H. Bahruji.

### References

- [1] Olah, G.A. (2005). Beyond Oil and Gas: The Methanol Economy. *Angewandte Chemie International Edition*, 44(18), 2636–2639, doi: 10.1002/anie.200462121
- [2] Behrens, M., Studt, F., Kasatkin, I., Kühl, S., Hävecker, M., Abild-Pedersen, F., Zander, S., Girsdsies, F., Kurr, P., Kniep, B.-L., Tovar, M., Fischer, R.W., Nørskov, J.K., Schlögl, R. (2012). The Active Site of Methanol Synthesis over Cu/ZnO/Al<sub>2</sub>O<sub>3</sub> Industrial Catalysts. *Science*, 336(6083), 893, doi: 10.1126/science.1219831
- [3] Speight, J.G. (2011). Chapter 8 - Hydrocarbons from Synthesis Gas. In J.G. Speight (Ed.), *Handbook of Industrial Hydrocarbon Processes* (pp. 281-323). Gulf Professional Publishing. doi: 10.1016/B978-0-7506-8632-7.10008-8
- [4] Kattel, S., Ramírez, P.J., Chen, J.G., Rodriguez, J.A., Liu, P. (2017). Active sites for CO<sub>2</sub> hydrogenation to methanol on Cu/ZnO catalysts. *Science*, 355(6331), 1296, doi: 10.1126/science.aal3573
- [5] Jiang, X., Koizumi, N., Guo, X., Song, C. (2015). Bimetallic Pd–Cu catalysts for selective CO<sub>2</sub> hydrogenation to methanol. *Applied Catalysis B: Environmental*, 170–171, 173–185, doi: 10.1016/j.apcatb.2015.01.010
- [6] Edwards, J.H. (1995). Potential sources of CO<sub>2</sub> and the options for its large-scale utilisation now and in the future. *Catalysis Today*, 23(1), 59–66, doi: 10.1016/0920-5861(94)00081-C
- [7] Bahruji, H., Guan, S., Puthiyapura, V.K. (2016). Precious Metal Catalysts for Sustainable Energy and Environmental Remediation. In *Modern Developments in Catalysis* (pp. 211-251). World Scientific (Europe). doi: 10.1142/9781786341228\_0007
- [8] Saeidi, S., Najari, S., Fazlollahi, F., Nikoo, M.K., Sefidkon, F., Klemeš, J.J., Baxter, L.L. (2017). Mechanisms and kinetics of CO<sub>2</sub> hydrogenation to value-added products: A detailed review on current status and future trends. *Renewable and Sustainable Energy Reviews*, 80, 1292–1311, doi: 10.1016/j.rser.2017.05.204
- [9] Zhang, X., Liu, J.-X., Zijlstra, B., Filot, I.A.W., Zhou, Z., Sun, S., Hensen, E.J.M. (2018). Optimum Cu nanoparticle catalysts for CO<sub>2</sub> hydrogenation towards methanol. *Nano Energy*, 43, 200–209, doi: 10.1016/j.nanoen.2017.11.021
- [10] Bahruji, H., Bowker, M., Jones, W., Hayward, J., Ruiz Esquivias, J., Morgan, D.J., Hutchings, G.J. (2017). PdZn catalysts for CO<sub>2</sub> hydrogenation to methanol using chemical vapour impregnation (CVI). *Faraday Discussions*, 197, 309–324, doi: 10.1039/C6FD00189K
- [11] Bond, G.C. (2016). Hydrogenation by gold catalysts: an unexpected discovery and a current assessment. *Gold Bulletin*, 49(3), 53–61, doi: 10.1007/s13404-016-0182-8
- [12] Bahruji, H., Bowker, M., Hutchings, G., Dimitratos, N., Wells, P., Gibson, E., Jones, W., Brookes, C., Morgan, D., Lalev, G. (2016). Pd/ZnO catalysts for direct CO<sub>2</sub> hydrogenation to methanol. *Journal of Catalysis*, 343, 133–146, doi: 10.1016/j.jcat.2016.03.017
- [13] Hartadi, Y., Widmann, D., Behm, R.J. (2015). CO<sub>2</sub> Hydrogenation to Methanol on Supported Au Catalysts under Moderate Reaction Conditions: Support and Particle Size Effects. *ChemSusChem*, 8(3), 456–465, doi: 10.1002/cssc.201402645
- [14] Abdel-Mageed, A.M., Klyushin, A., Knop-Gericke, A., Schlögl, R., Behm, R.J. (2019). Influence of CO on the Activation, O-Vacancy Formation, and Performance of Au/ZnO Catalysts in CO<sub>2</sub> Hydrogenation to Methanol. *The Journal of Physical Chemistry Letters*, 10(13), 3645–3653, doi: 10.1021/acs.jpcclett.9b00925
- [15] Pawinrat, P., Mekasuwandumrong, O., Panpranot, J. (2009). Synthesis of Au–ZnO and Pt–ZnO nanocomposites by one-step flame spray pyrolysis and its application for photocatalytic degradation of dyes. *Catalysis Communications*, 10(10), 1380–1385, doi: 10.1016/j.catcom.2009.03.002
- [16] Derrouiche, S., La Fontaine, C., Thrimurtulu, G., Casale, S., Delannoy, L., Lauron-Pernot, H., Louis, C. (2016). Unusual behaviour of Au/ZnO catalysts in selective hydrogenation of butadiene due to the formation of a AuZn nanoalloy. *Catalysis Science & Technology*, 6(18), 6794–6805, doi: 10.1039/C5CY01664A
- [17] Borissov, D., Pareek, A., Renner, F.U., Rohwerder, M. (2010). Electrodeposition of Zn and Au–Zn alloys at low temperature in an ionic liquid. *Physical Chemistry Chemical Physics*, 12(9), 2059–2062, doi: 10.1039/B919669B

- [18] Wang, T., Jin, B., Jiao, Z., Lu, G., Ye, J., Bi, Y. (2014). Photo-directed growth of Au nanowires on ZnO arrays for enhancing photoelectrochemical performances. *Journal of Materials Chemistry A*, 2(37), 15553–15559, doi: 10.1039/C4TA02960G
- [19] Bahruji, H., Armstrong, R.D., Ruiz Esquiús, J., Jones, W., Bowker, M., Hutchings, G.J. (2018). Hydrogenation of CO<sub>2</sub> to Dimethyl Ether over Brønsted Acidic PdZn Catalysts. *Industrial & Engineering Chemistry Research*, 57(20), 6821–6829, doi: 10.1021/acs.iecr.8b00230
- [20] Bahruji, H., Esquiús, J.R., Bowker, M., Hutchings, G., Armstrong, R.D., Jones, W. (2018). Solvent Free Synthesis of PdZn/TiO<sub>2</sub> Catalysts for the Hydrogenation of CO<sub>2</sub> to Methanol. *Topics in Catalysis*, 61(3), 144–153, doi: 10.1007/s11244-018-0885-6
- [21] Shen, W.J., Jun, K.W., Choi, H.S., Lee, K.W. (2000). Thermodynamic Investigation of Methanol and Dimethyl Ether Synthesis from CO<sub>2</sub> Hydrogenation. *Korean Journal of Chemical Engineering*, 17(2), 210–216, doi: 10.1007/BF02707145
- [22] Sholeha, N.A., Jannah, L., Rohma, H.N., Widiastuti, N., Prasetyoko, D., Jalil, A.A., Bahruji, H. (2020). Synthesis of Zeolite Nay from Dealuminated Metakaolin as Ni Support for CO<sub>2</sub> Hydrogenation to Methane. *Clays and Clay Minerals*, 68(5), 513–523, doi: 10.1007/s42860-020-00089-3
- [23] Guilera, J., del Valle, J., Alarcón, A., Díaz, J.A., Andreu, T. (2019). Metal-oxide promoted Ni/Al<sub>2</sub>O<sub>3</sub> as CO<sub>2</sub> methanation micro-size catalysts. *Journal of CO<sub>2</sub> Utilization*, 30, 11–17, doi: 10.1016/j.jcou.2019.01.003
- [24] Strunk, J., Kähler, K., Xia, X., Comotti, M., Schüth, F., Reinecke, T., Muhler, M. (2009). Au/ZnO as catalyst for methanol synthesis: The role of oxygen vacancies. *Applied Catalysis A: General*, 359(1), 121–128, doi: 10.1016/j.apcata.2009.02.030